Mutagenesis vol. 24 no. 5 pp. 439–445, 2009
Advance Access Publication 15 July 2009
doi:10.1093/mutage/gep027

Genotoxicity and morphological transformation induced by cobalt nanoparticles and cobalt chloride: an *in vitro* study in Balb/3T3 mouse fibroblasts

Jessica Ponti*, Enrico Sabbioni[1], Barbara Munaro[1], Francesca Broggi, Patrick Marmorato, Fabio Franchini, Renato Colognato and François Rossi

Nanobiosciences Unit and [1]*In-vitro* Methods Unit, European Commission, Joint Research Centre, Institute for Health and Consumer Protection, Via E. Fermi 2749, 21027 Ispra (VA), Italy

Nanotechnology is an emerging field that involves the development, manufacture and measurement of materials and systems in the submicron to nanometer range. Its development is expected to have a large socio-economical impact in practically all fields of industrial activity. However, there is still a lack of information about the potential risks of manufactured nanoparticles for the environment and for human health. In this work, we studied the cytotoxicity, genotoxicity and morphological transforming activity of cobalt nanoparticles (Co-nano) and cobalt ions (Co^{2+}) in Balb/3T3 cells. We also evaluated Co-nano dissolution in culture medium and cellular uptake of both Co-nano and Co^{2+}. Our results indicated dose-dependent cytotoxicity, assessed by colony-forming efficiency test, for both compounds. The toxicity was higher for Co-nano than for Co^{2} after 2 and 24 h of exposure, while dose–effect relationships were overlapping after 72 h. Statistically significant results were observed for Co-nano with the micronucleus test and the comet assay, while for Co^{2+} positive results were observed only with the latter. In addition, even when Co-nano was genotoxic (at >1 μM), no evident dose-dependent effect was observed. Concerning morphological transformation, we found a statistically significant increase in the formation of type III foci (morphologically transformed colonies) only for Co-nano. Furthermore, we observed a higher cellular uptake of Co-nano compared with Co^{2+}.

Introduction

Nanotechnology is a rapidly emerging field that involves the development, manufacture and measurement of materials and systems from the submicrometer to nanometer range. This pervasive technology is expected to have a large economic and social impact in almost all sectors of industrial and scientific activity. Furthermore, the unique and diverse physicochemical properties of nanoscale materials suggest that toxicological properties may differ from the corresponding bulk materials (1).

Potential occupational and public exposure, through inhalation, oral ingestion, dermal absorption or by injection, of manufactured nanoparticles, with particles size $\leq$100 nm, will probably increase in the near future, due to the ability of nanomaterials to improve the quality and performance of many consumer products, as well as the development of therapeutic strategies and tests. However, there is still a lack of information about the impact on environment and on human health of manufactured nanoparticles as well as reliable data on risk assessment (2).

In this context, the European Commission, through the Communication 'Towards a European Strategy for Nanotechnology' in combination with the 'European Action Plan for Nanosciences and Nanotechnologies' (3), suggests a safe and responsible strategy to reinforce the European Union's leading position in this Research and Development area, calling for increasing research using appropriate methods to assess the toxicological profile of manufactured nanoparticles. In particular, *in vitro* systems that could reduce, refine and replace animal methods (4) are recommended to understand the mechanisms of action of manufactured nanoparticles (e.g. intracellular trafficking, metabolism, toxicological profile and morphological transformation).

To support this strategy, the Joint Research Centre of the European Commission has developed in the last 2 years a research plan on nanoparticles toxicology based on an integrated approach, combining cell-based *in vitro* assays with specific radiochemical and physicochemical facilities (5). The experimental approach consists of the selection of manufactured nanoparticles to be studied, based on industrial interest, the assessment of their physicochemical characterization and their testing to assess their toxicological profiles using *in vitro* systems relevant for human exposure. In the present work, we studied cobalt nanoparticles (Co-nano) because of their industrial interest. In fact, metallic cobalt (Co(0)), as nanoparticles, is used in biology and medicine in different forms from the simplest, such as cobalt oxide, to complex organic compounds or biopolymers (6,7). Cobalt was used in this work as a 'model' to study nanoparticle toxicology also because of the possibility to radiolabel it. In this work, in particular, we studied the cytotoxicity, morphological transforming activity and genotoxicity of Co-nano and cobalt chloride (Co^{2+}) in Balb/3T3 cells. By using radiolabelled compounds (^{60}Co-nano and $^{57}Co^{2+}$), we also studied Co-nano behaviour in cell culture medium and Co-nano and Co^{2+} uptake by cells.

We selected the Balb/3T3 model because it is one of the *in vitro* systems recently considered at the European Centre of Validation of Alternative Methods (ECVAM) for prevalidation exercises evaluating the cytotoxicity and morphological transformation of chemicals (8). This model has been applied at ECVAM as a screening test for several metal compounds (9) and this is the first attempt to apply this methodology in nanoparticle studies.

Materials and methods

Chemicals and radioactive compounds

Cobalt (II) chloride [$CoCl_2$ (7791-13-1)] was supplied by Alfa, Karlsruhe, Germany; Co-nano, which refer to metal nanoparticles Co(0) (20 nm <

*To whom correspondence should be addressed. Tel: +39 0332785793; Fax: +39 0332785787; Email: jessica.ponti@jrc.it

Co-nano < 500 nm), were supplied by Laboratory of Biomaterials, University of Modena and Reggio Emilia, Modena, Italy.

Cobalt chloride was dissolved in ultrapure water at a concentration of 10 mM. The freshly prepared stock solution was sterilized using a 0.2 μm filter (Millipore, Italy) and diluted in complete culture medium to give final concentrations in the range of 1–100 μM.

Co-nano were suspended in ultrapure sterile water at the concentration of 10 mM. Freshly prepared stock suspensions of Co-nano were washed by centrifugation (13 000× *g* for 30 min) to remove the Co^{2+} that arose from nanoparticles synthesis (10–15% of the initial concentration); they were ultrasonicated for 15 min and immediately diluted in complete culture medium to give test concentrations in the range of 1–100 μM.

The compounds were analysed for the elemental impurities by Inductively Coupled Plasma Mass Spectrometry (Perkin-Elmer SCIEX, Ontario, Canada). The results of the analysis (data not shown) indicated a degree of purity suitable to avoid any possible artefacts for cytotoxicity, morphological transformation and genotoxicity induced in our *in vitro* system (9).

Co-nano were characterized in water and in complete culture medium for their morphology by scanning electron microscope/energy dispersive using X-ray (SEM-EDX) technique and size distribution by nanoparticles tracking analysis (NanoSight LM20 Nanoparticles Analysis System, Salisbury, UK). Samples for SEM analysis were prepared depositing 20 μl of a 10 mM Co-nano suspension in water or culture medium on silicon substrate (0.5 × 0.5 cm). Drops were dried for 2 h under an infrared lamp and immediately analysed. Co-nano size analyses were performed by injecting a fresh prepared stock suspension (10 mM) both in water and complete culture medium.

$^{57}Co^{2+}$ was supplied by Amersham Biosciences (Milan, Italy). It was added to stable Co^{2+} (10 mM) to obtain $^{57}Co^{2+}$ at concentrations in the range of 10–100 μM. The solutions were equilibrated for 10 min at room temperature before their use. ^{60}Co-nano were prepared through irradiation of Co-nano powder in a high flux nuclear reactor (HFR, Petten, Netherland) by a thermal neutron flux of 2×10^{14} neutrons/cm^2/sec. Testing suspensions were prepared as described above for unlabelled Co-nano and added to culture medium to give concentrations of 10, 20 and 100 μM. Radioactivity was measured by an automatic γ-counting system (Wallac 1480, Wallac Oy, Turku, Finland) equipped with a well-type NaI (TI) detector and using the characteristic line of 800–2000 keV (^{60}Co-nano) and 50–800 keV (^{57}Co) photon emission.

Cobalt ion leakage from Co-nano in culture medium

The concentration of radiolabelled Cobalt ions ($^{60}Co^{2+}$), released from Co-nano suspensions, was measured by a γ-counter. We prepared samples by diluting the stock ^{60}Co-nano suspension in complete culture medium as described to concentrations of 10 and 100 μM. We incubated them for 2, 24 and 72 h under standard cell culture conditions (37°C, 5% CO_2, 95% humidity).

After incubation, aliquots (1 ml) of particles' suspensions were ultracentrifuged [105 000× *g* for 90 min, Optima MAX 130 000 r.p.m. (Beckman, Midland, ON, Canada)] and the supernatant containing $^{60}Co^{2+}$ was collected and measured. Results were expressed as percentage of tested suspensions (10 and 100 μM) ± SD.

Balb/3T3 cell line and cell culture conditions

Balb/3T3 mouse fibroblasts stemming from the clone A31-1-1 were purchased from the Istituto Zooprofilattico Sperimentale dellaLombardia e dell'Emilia, Brescia, Italy. Cells were supplied with mycoplasma free and source certification. Experimental cultures were prepared from deep-frozen stock vials and always kept in a subconfluent state. They were maintained in complete culture medium prepared using Dulbecco's modified Eagle's medium low glucose (Gibco, Invitrogen Corporation, Milan, Italy) containing 10% v/v of semi-synthetic Foetal Clone Serum III (Hyclone, Celbio, Milano, Italy), 4.8 mM of L-glutamine (200 mM), 1% v/v of Fungizone liquid (250 μg/ml), 0.6% v/v of penicillin–streptomycin (10000 U/ml penicillin and 10000 U/ml streptomycin, Gibco) and passaged at 1:15 ratio, using trypsin–ethylenediaminetetraacetic acid (1×) (Gibco). Cell preparations were maintained in standard cell culture conditions (37°C, 5% CO_2 and 95% humidity) (10).

Concurrent cytotoxicity and morphological transformation assay

The Balb/3T3 cell transformation assay (CTA) has been carried out by assessing the concurrent cytotoxicity and morphological transformation in terms of colony-forming efficiency (CFE) and formation of type III foci, respectively (11).

Cytotoxicity

CFE assay was used to study cytotoxicity induced by Co-nano and Co^{2+} at 2, 24 and 72 h of exposure that correspond to the exposure time for comet assay, micronucleus test and morphological transformation assay (CTA), respectively. Cells were seeded at the density of 200 cells per dish in 4 ml complete culture medium (60 × 15 mm Petri dish, Corning-Costar, Milan, Italy, six replicates each treatment). After 24 h, medium was changed and 4 ml of fresh medium containing the compound to be tested was added to obtain the appropriate final cobalt concentrations ranging from 0.1 to 100 μM. After 2, 24 or 72 h of exposure, dishes were fed with the complete culture medium and 7 days later, the cells were fixed with 3.7% v/v of formaldehyde solution (Sigma-Aldrich, Milan, Italy) in phosphate-buffered saline (PBS) (1×) without calcium, magnesium and sodium bicarbonate (Gibco) and stained with 0.4% v/v Giemsa solution (Sigma-Aldrich) in ultrapure water. Colonies were manually scored under a stereomicroscope. The results were expressed as CFE (%) [(average of treatment colonies/average of control colonies) ×100] and the corresponding standard error mean [$SEM\ \% = SD/\sqrt{}$(number of treatments)]. IC50 values were interpolated graphically from the dose–effect curves.

Morphological transformation assay

A total of 1.5×10^3 cells/ml in 10 ml of complete culture medium were seeded in each dish (100 × 20 mm Petri dish, Corning-Costar, 10 replicates each treatment). After 24 h, the medium was changed to those containing selected concentrations of Co-nano or Co^{2+} previously interpolated by the CFE graphs. In particular, we used 1, 7, 10 and 30 μM for Co-nano and 1, 7, 30 and 70 μM for Co^{2+} corresponding to IC20, 30, 50 and 80. Sodium chromate at 50 μM·[$Na_2CrO_4 \cdot 4H_2O$ (10034-82-9), Alfa Aesar, Milano, Italy] was used as a positive control (12,13).

After treatment, the cultures were maintained for 5 weeks, with the culture renewed twice a week and at the end of the experiment the cells were fixed and stained, as reported above for the CFE assay. Type III foci were manually scored for morphological transformation under stereomicroscope as described by the International Agency for Cancer Research (IARC) Working Group (14).

Transformation results were expressed as the probability of a neoplastic event per surviving cell (15,16). The amount of surviving cell fraction was calculated as the percentage of cells remaining plated after seeding and surviving after treatment at the given dose. The transformation frequency (T_f) was expressed using the formula $T_f = [A/(B \times C \times D)]$, where A = total number of type III foci per treatment, B = CFE(%)/100, C = Plating Efficiency (%)/100, D = cell seeded × no. of plates, where Plating Efficiency (%) = number of colonies formed in the control × 100/200 and 200 is the total number of cells seeded in one CFE dish (15,16).

Experimental data were analysed by Fisher's exact test (15–17) considering the number of type III foci in the treatments and the surviving cells compared to the corresponding negative control (untreated cells). Only $P < 0.05$ was considered statistically significant.

Comet assay

A total of 1.5×10^5 cells/ml in 4 ml of complete culture medium were seeded in a six-well cell culture plate (Falcon, Milan, Italy). After 24 h, cells were treated for 2 h with 4 ml of suspensions of Co-nano and Co^{2+} at subtoxic concentrations (1, 3 and 5 μM), previously interpolated from CFE assay. Cells were also exposed for 2 h at 300 μM H_2O_2 (Sigma–Aldrich) as positive control. After exposure, cells were washed twice with 4 ml PBS and harvested in the 50 ml tube together with the medium of the treatment (12 ml in total). The comet assay was performed according to the method described by Singh *et al*. (18) with some modifications as follows. Conventional slides were coated with a first layer of 150 μl of 0.5% Normal Melting Point Agarose (Sigma–Aldrich), dried for 10 min at 65°C and spread with a coverslip. After solidification for 10 min at 4°C and removal of the coverslip, 75 μl of 0.5% low melting point agarose (LMA) (Sigma–Aldrich) was mixed with $\sim 6 \times 10^4$ cells suspended in 20 μl and layered onto the slides, covered and kept for 15 min at 4°C. Then the coverslips were removed and the slides were covered with a third layer of 75 μl LMA. After the solidification of the agarose (4°C, 15 min), the coverslips were removed and the slides were immersed for 1 h at 4°C in cold fresh lysing solution (2.5 M NaCl, 100 mM Na_2EDTA, 10 mM Tris, pH 10) containing 1% Triton X-100 and 10% dimethylsulfoxide. Two slides were prepared from each control and treatment group. To avoid the occurrence of additional DNA damage, the following steps were performed at 4°C under dim light. The slides were placed for 20 min in horizontal gel electrophoresis unit filled with electrophoresis cold buffer (300 mM NaOH, 1 mM Na_2EDTA, pH 13.5). After electrophoresis (20 min at 0.73 V/cm and 300 mA), the slides were washed twice for 5 min with neutralizing buffer (0.4 M Tris, pH 7.5) and fixed with absolute ethanol (Carlo-Erba, Milan, Italy) for 3 min. The slides were stained with 50 μl ethidium bromide (0.4 μM/ml; Sigma–Aldrich) just before analysis.

Analysis was made using the Komet 3.1 Image Analysis System (Kinetic Imaging Ltd, Liverpool, UK) fitted with an Olympus Bx50 fluorescence microscope with the following settings: magnification ×200, wide band excitation filter 480–550 nm and barrier filter 590 nm.

Experimental data were analysed according to Duez *et al*. (19) using one-way analysis of variance (ANOVA) (Graph Pad Prism 4) to estimate the

significance of DNA damage. Four runs per treatment and 25 cells per run were analysed. The parameter considered as the end point of the experiment was the percentage of DNA in the tail of the comet and the median was extracted for each run. The four median treatments were tested with one-way ANOVA test. Given an overall ANOVA $P < 0.05$, a post hoc Dunnett's test was applied to compare the treatments against the negative control.

Micronucleus test

A total of 7.5×10^4 cells/ml in 4 ml of complete culture medium were seeded in every well of a six-well cell culture plate (FALCON). After 24 h, cells were treated for 24 h with 4 ml of suspensions of Co-nano and solutions of Co^{2+} at 1, 5 and 10 μM previously interpolated from CFE assay and corresponding maximum to IC50. Positive control was mitomycin C (Sigma–Aldrich) at 0.5 μM.

After treatment, cells were incubated with fresh medium containing cytochalasin B (Sigma–Aldrich) (4.5 μg/ml) for 24 h. Cells were washed twice with 4 ml PBS harvested in a 50 ml tube (FALCON) and centrifuged at 200× *g* for 5 min. A solution of methanol/acetic acid (3:5) was added to the cell pellet and subsequently centrifuged at 200× *g* for 5 min. Cells were suspended with 5 ml methanol and kept at −20°C for 24 h. Tubes were then centrifuged at 300× *g* for 5 min and fixed twice with a solution of methanol/acid acetic (6:1). Cells were spotted on a glass slide and stained with Giemsa solution (diluted 2:100 in water) for 30 min.

The results were analysed by calculating the binucleated micronucleated cells frequency as the number of binucleated cells containing one or more micronuclei per 1000 binucleated cells (20).

Statistical analysis was performed by Fisher's exact test and the differences were considered statistically significant at $P < 0.05$ (17).

Uptake

A total of 10^5 cells/ml in 10 ml of complete culture medium were seeded in a 75 cm^2 flask (Corning-Costar). After 24 h, cells were treated with suspensions of ^{60}Co-nano and solutions of $^{57}Co^{2+}$ for 2, 24 and 72 h at concentrations corresponding to IC50 at different exposure times previously interpolated by the CFE graphs. In particular, we exposed the cells to 10 and 20 μM of ^{60}Co-nano and 10, 20 and 100 μM of $^{57}Co^{2+}$. After exposure, cells were washed twice with 10 ml PBS, detached with 1 ml trypsin solution and harvested with 10 ml complete culture medium. Cells were counted, centrifuged (200× *g* for 5 min) and washed twice with PBS. Radioactivity was directly analysed in the pellet treated with $^{57}Co^{2+}$. The majority of nanoparticles not bound to cells were removed with the two washes of adherent cells in the flask, while for the others (e.g. nanoparticles on the membrane but not inside the cells), we separated them using a percoll gradient (10% v/v NaCl 1.5 M, Sigma–Aldrich; 48% v/v percoll, Amersham Health Care GE, Milan, Italy; 42% v/v ultrapure water; 20 000× *g* for 15 min). Cells were then suspended in 1 ml PBS and put on 2 ml of percoll gradient. After centrifugation, three bands were analysed and the cells in the first band were counted for the number of cells and ^{60}Co-nano uptake.

Results

In this work, we report the cytotoxicity, genotoxicity and the morphological transforming activity of metallic Co-nano compared to its soluble form [cobalt ions (Co^{2+})].

The physicochemical characterization of the Co-nano was carried out verifying morphology, size distribution and nanoparticle behaviour in culture medium. Scanning electron microscope (SEM) analysis showed nanoparticles aggregate both in water and in complete culture medium. The nanoparticle tracking analysis instead showed a size distribution ranging between 20 and 500 nm with a peak at 80 nm (Figure 1).

The release of $^{60}Co^{2+}$ in complete culture medium was analysed by γ-counter after 2, 24 and 72 h of incubation (Figure 2). The results obtained showed a time-dependent increase in the percentage of $^{60}Co^{2+}$ release varying from 9 up to 31% and from 7 to 44% when 10 or 100 μM, respectively, of Co-nano were tested (Figure 2).

Cytotoxicity was evaluated by CFE test. Figure 3 shows dose-dependent responses obtained for Co-nano and Co^{2+} after 2, 24 and 72 h of exposure. The graphical representation shows the mean values of the percentage of the control obtained from three independent experiments, with six replicates for each concentration, with the corresponding *SEM*. The data indicate a dose-dependent cytotoxicity for both compounds. The toxicity was higher for Co-nano than for to Co^{2+} after 2 and

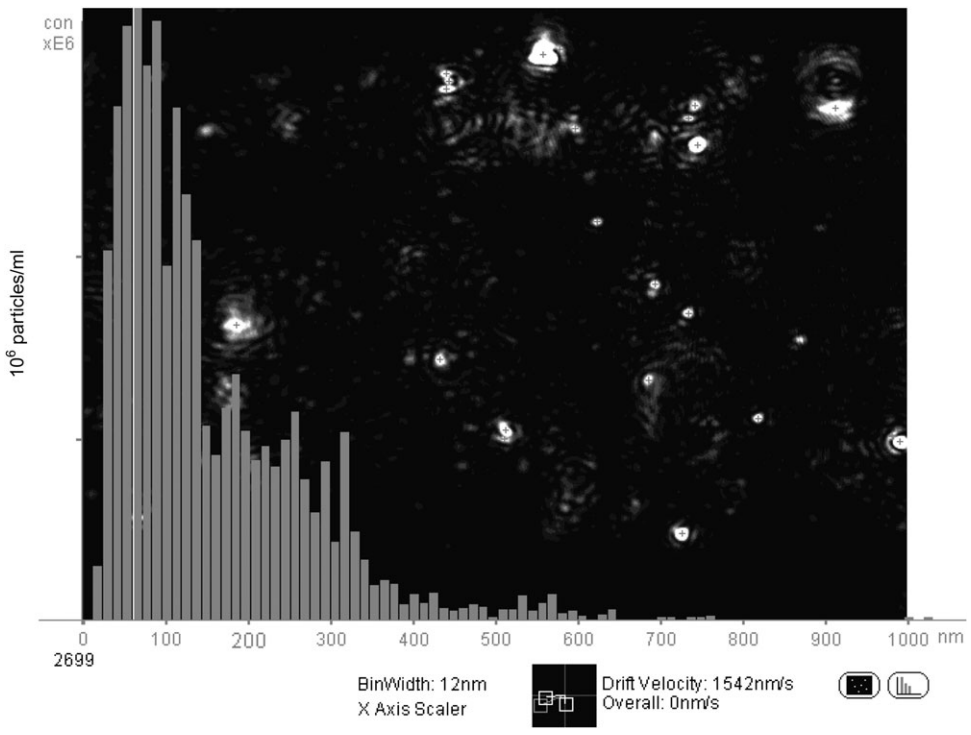

Fig. 1. Nanoparticles size distribution by nanoparticles tracking analysis (Nanosight) of Co-nano suspension (10 mM) in water. Size distribution shows a peak at 80 nm and provides a quantitative result from the qualitative image that shows polydispersed particles.

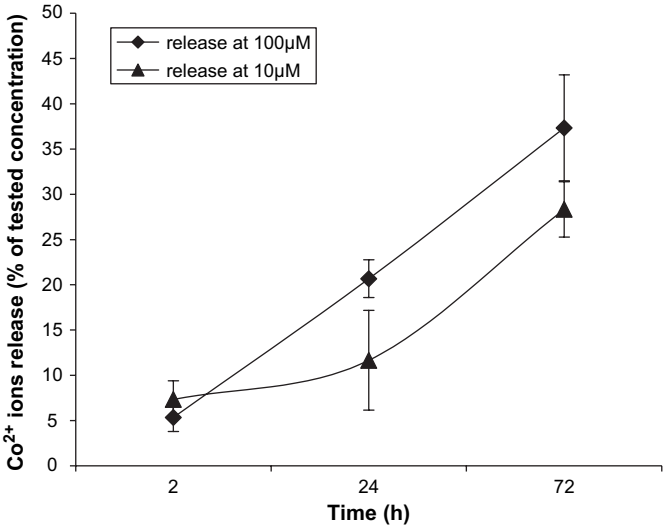

Fig. 2. Percentage of Co^{2+} ions released from 10 μM (closed triangles) and 100 μM (closed diamonds) of Co-nano after 2, 24 and 72 h of incubation in cell culture medium measured by γ-counter. Data represent the mean of three experiments ± SD.

24 h of exposure, while dose–effect relationships were overlapping after 72 h.

To study the morphological transforming activity of Co-nano and Co^{2+}, we selected concentrations ranging from 1 to 30 μM and from 1 to 70 μM, respectively (Table I). These concentrations correspond to IC20, 30, 50 and 80. The results show that Co-nano were cytotoxic and an increase in morphological transformation, expressed as T_f, was observed for all the concentrations tested (except for Co-nano at 1 μM); while Co^{2+} was cytotoxic but no statistically significant morphological transformation was observed (Table I).

Genotoxicity was assessed both by analysing induction of primary DNA damage, triggered by the formation of single- and double-strand breaks by comet assay, and by evaluating the presence of fixed mutational lesions performed by micronucleus test (Figure 4 and Table II). Figure 4 shows a statistically significant induction of DNA damage for both Co-nano and Co^{2+} (Figure 4) exposed to subtoxic concentrations (1, 5 and 10 μM). The data show that the increase of DNA damage for Co-nano was not dose dependent (Figure 4, grey boxes), whereas for Co^{2+}, although exerting a comparable genotoxic response, dose-dependent behaviour (Figure 4, white boxes) was observed.

The micronucleus test (Table II) performed using different doses (1, 5 and 10 μM), corresponding to IC50, shows for Co-nano a statistically significant induction ($P < 0.001$) of chromosomal aberrations at all the concentrations tested, but it was not dose dependent, whereas for Co^{2+} under the same experimental conditions, no genotoxic effect was observed (Table II).

In order to verify that the biological results obtained were due to internalization of nanoparticles, we studied the uptake rate of ^{60}Co-nano and $^{57}Co^{2+}$ after 2, 24 and 72 h of exposure at the corresponding IC50. The uptake analysis at the IC50 values was performed in order to normalize the results at the same percentage of viable cells. Table III shows the uptake rate for ^{60}Co-nano in comparison to $^{57}Co^{2+}$. There was a difference between the two compounds tested with an ∼50- to 100-fold increase for Co-nano.

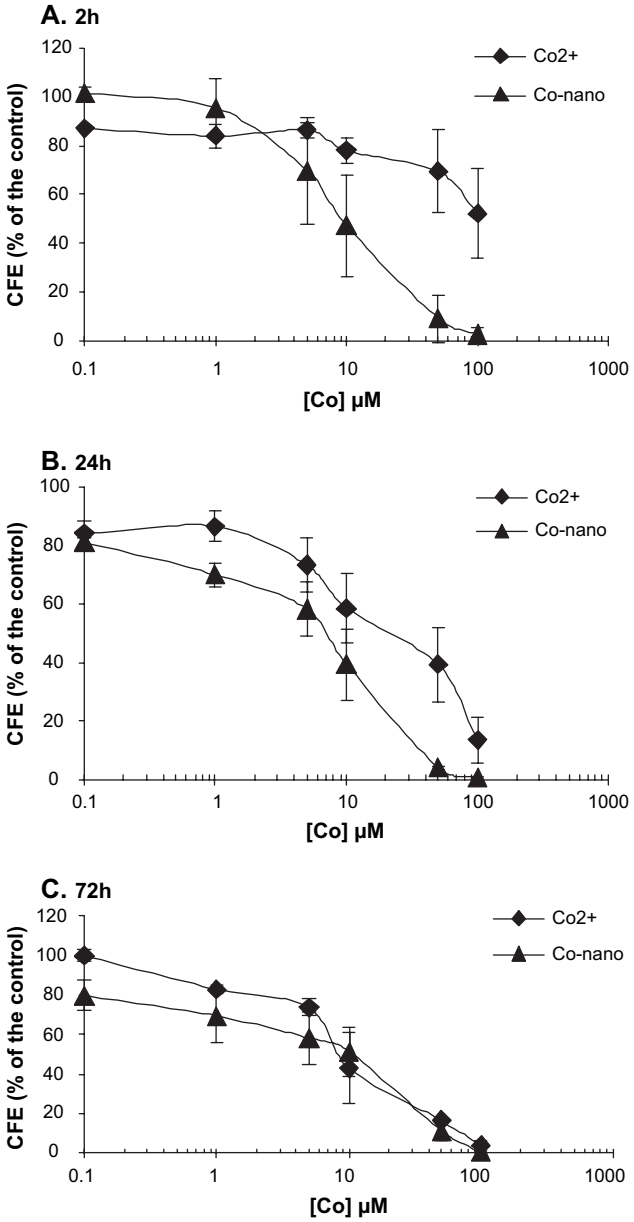

Fig. 3. Cytotoxicity, expressed as CFE (% of the control) ± *SEM*, induced in Balb/3T3 cell lines by Co^{2+} (closed diamonds) and Co-nano (closed triangles) after 2, 24 and 72 h of exposure (**A**, **B**, and **C**, respectively). Curves are obtained as average of three experiments, six replicates each treatment.

Discussion

The toxicology and morphological transforming activity of manufactured nanoparticles still remain open questions in the scientific community. It has been demonstrated in different *in vitro* and *in vivo* studies that the manufactured nanoparticles possess the ability to be internalized into cells inducing inflammatory response (21) in relation to their size, shape and surface areas (22).

Moreover, studies of ultrafine particle inhalation suggest that particle size can have a higher impact on toxicity than other physicochemical characteristics, due principally to the large surface area and its reactivity (21,23). If surface reactivity is influenced by the size of the particle, the surface properties can be changed by coating nanoparticles with different materials. This interaction of surface area and particle composition in

Table I. Concurrent cytotoxicity and morphological transformation induced by Co^{2+} and Co-nano after 72 h of exposure

Compound	μM	CFE[a] (%)	PE (%)	Survived cells	Type III foci (total)	T_f ($\times 10^{-4}$)	*P*
Control	–	100	24.7	49 400	1	0.20	–
$Na_2CrO_4 \cdot 4H_2O$	50	38	52.5	39 600	21	5.3	<0.001
Co^{2+}	1	86	46	59 340	2	0.33	NS
Co^{2+}	7	76	46	52 440	4	0.76	NS
Co^{2+}	30	47	24.5	23 030	1	0.43	NS
Co^{2+}	70	15	24.5	7350	0	0	
Co-nano	1	98	24.7	48 412	2	0.41	NS
Co-nano	7	75	46	51 750	10	1.93	<0.01
Co-nano	10	52	24.7	25 688	4	1.56	<0.05
Co-nano	30	24	46	16 560	11	6.64	<0.001

PE, plating efficiency; NS, not significant.
[a]Average of three experiments, six replicates each concentration.

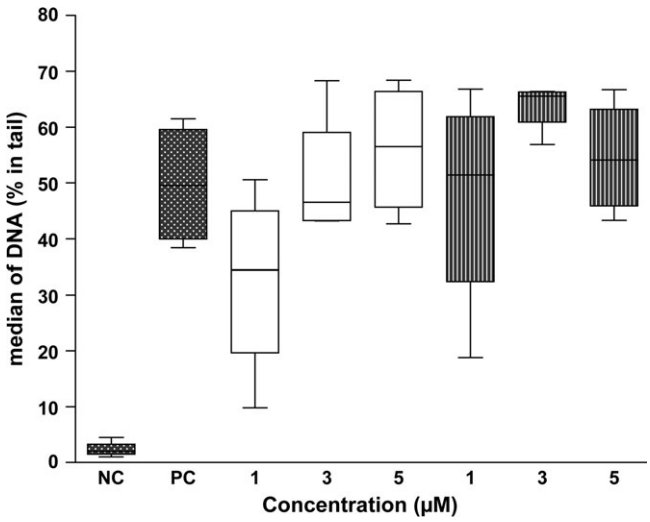

Fig. 4. DNA damage induced after 2 h of exposure to subtoxic concentrations (1–5 μM) of Co-nano (grey boxes) and Co^{2+} (white boxes) in Balb/3T3. Statistical significance (ANOVA): $P < 0.01$ for each treatment. NC, negative control; PC, positive control H_2O_2 300 μM.

eliciting biological responses adds an extra dimension of complexity to evaluating the potential of adverse effects that may result from exposure to these materials (24). There are indications in the literature that manufactured nanoscale materials may distribute in the body in unknown ways and certain nanoparticles have been observed to accumulate preferentially in different subcellular organelles (6).

In this work, we selected Co-nano for the analysis of the possible cytotoxicity, genotoxicity and morphological transforming activity together with an evaluation of the uptake rate of this nanoparticle type in a selected cell model. Furthermore, we decided to investigate the biological effects of well-characterized nanoparticles, taking into account their size distribution and the stability in culture medium in forms of Co^{2+} leakage. In fact, a large amount of metallic manufactured nanoparticles (e.g. $CoFe_2O_4$) produced by industry for different applications (25,26) is synthesized without any coating procedure, and in many cases, they naturally aggregate and agglomerate, thereby changing their size, and they tend to release in aqueous solvents their corresponding ions, natural effects of a solvatation by solvent due to dissolution. The study

Table II. Frequency of micronucleated binucleated cells induced by Co^{2+} and Co-nano after 24 h of exposure

Compound	μM	BNMN/‰[a]	*P*
Control	–	24	
Mitomycin C	0.5	203	<0.001
Co^{2+}	1	28	NS
Co^{2+}	5	28	NS
Co^{2+}	10	31	NS
Co-nano	1	106	<0.001
Co-nano	5	53	<0.001
Co-nano	10	44	<0.05

NS, not significant.
[a]BNMN/‰: binucleated micronucleated cells containing one or more micronuclei per 1000 binucleated cells.

Table III. Uptake of $^{57}Co^{2+}$ and ^{60}Co-nano in Balb/3T3 cells after 2, 24 and 72 h of exposure to the corresponding IC50

Compound	Exposure time (h)	IC50 (μM)	Uptake (fgCo cell-1)
$^{57}Co^{2+}$	2	100	16
	24	20	7
	72	10	7
^{60}Co-nano	2	20	990
	24	10	250
	72	10	290

of these aspects is fundamental for understanding their *in vitro* biological effects and potential toxicity (27,28).

For this reason, we analysed the time-dependent chemical release of Co^{2+} in culture medium (Figure 2). The data show that there is a time-dependent increase in Co^{2+} release for both the concentrations tested, reaching 44% for 100 μM at 72 h. Based on the cytotoxicity results obtained, we can speculate that, in these experimental conditions, the concentration of Co^{2+}, extrapolated by the percentage of Co^{2+} released in Figure 2, is not enough to justify the observed Co-nano toxicity (Figure 3). In fact, for example, considering an exposure time of 2 h at the concentration of 100 μM Co-nano that correspond to a 7% Co^{2+} release (7 μM), we observed no cell viability for Co-nano, whereas there was 80% cell viability for Co^{2+}. Consequently, the cytotoxic effect seems likely to be induced by nanoparticles and not by Co^{2+} although a complementary and/or a synergic effect cannot be excluded.

Concerning the morphological transformation by cobalt and its compounds, the IARC (29) concluded that cobalt and its compounds are possibly carcinogenic to humans (Group 2B) since there was sufficient evidence in experimental animal studies but inadequate evidence for carcinogenicity in humans (lung cancer) (30).

In our *in vitro* study, Co-nano (Table I) showed a dose-dependent statistically significant increase in morphological transforming activity, expressed as T_f, ranging from 0.41×10^{-4} to 6.64×10^{-4} for 1–30 μM, respectively. A statistically significant increase in the end point was also observed if the single dose value data were analysed versus control ($P < 0.01$), starting from 7 μM (Table I). For cobalt chloride (Table I), in contrast, no statistically significant increase, either for the dose dependency or for the single concentration values versus control, was observed. This latter evidence is also supported by Lison *et al.* (31), who demonstrated a genotoxic potential for cobalt *in vitro* without evidence for morphological transforming potential (31).

Analysing the genotoxicity effects, there are few data reporting induction of damage at the DNA level, but almost all are related to cobalt metal or compounds in the soluble forms, whereas for Co-nano, data are still missing or sparse. De Boeck *et al*. (32) explored the *in vitro* genotoxicity of Co metal and compared it with that of hard metal particles in terms of concentration and time dependency. Co metal and cobalt chloride produced approximately the same level of DNA damage. Recently, DNA migration (alkaline comet assay) in human lymphocytes after treatment with different combinations of Co metal and metallic carbide particles was assessed by Lison *et al*. (33). De Boeck *et al*. (32) assessed the ability of powder mixtures of Cr_3C_2, Mo_2C and NbC with cobalt to induce chromosome/genome mutations (micronucleus test) in human lymphocytes. The exact mechanism by which cobalt compounds induce micronuclei is not clear; it might be the consequence of the direct clastogenic activity, but an aneuploidogenic activity should not be overlooked given the literature data on cobalt (II) (34).

Concerning this specific type of toxicity, our data (Figure 4) demonstrate that for both Co-nano and Co^{2+}, there was a statistically significant increase ($P < 0.01$) in the induction of single-strand and double-strand breaks (Figure 4). Analysing the genotoxic potential in terms of chromosomal aberrations (Table II), we observed a statistically significant ($P < 0.001$) increase, not dose dependent, in the frequency of micronucleated binucleated cells for Co-nano but not for Co^{2+} (Table II). In addition, for Co-nano, we observed lower values in the number of micronucleated binucleated cells at the higher concentrations (100 μM), in comparison with the lower dose tested (1 μM). This latter effect is likely to be due to the cytotoxicity effect (Figure 3) masking the genotoxic potential. Briefly, an increase in cytotoxicity is counteracted by a decrease in the genotoxicity.

The different behaviour of the two cobalt forms likely suggests that Co-nano is a potential genotoxic carcinogen. In fact, the formation of chromosomal aberrations, in the form of micronuclei, induced in this study by Co-nano, is a process which leads to a stable mutation that with higher probability could trigger morphological transformation. In contrast, the production of DNA damage, in the form of single- and double-strand breaks, for example induced by Co^{2+}, is a premutagenic lesion, easily removed by molecular repair processes, not necessarily reflecting the fact that the cells will undergo morphological transformation. Regarding the genotoxicity effects of nanoparticles, the data are sparse and have to be well evaluated considering the different types of *in vitro* models. In fact, a study on Co-nano, by Colognato *et al*. (35), using both the alkaline comet assay and the micronucleus test, shows that in human peripheral leukocytes, there is evident dose-dependent increase in the primary DNA damage for Co-nano but not for Co^{2+}, whereas analysing the frequency of micronucleated binucleated cells, both the compounds show positive results.

Looking at the relevant biological effects observed by all our assays, we decided to investigate the cellular uptake of Co-nano. Results showed a 50- to 100-fold increased uptake for ^{60}Co-nano compared with $^{57}Co^{2+}$ (Table III). This high quantity of Co-nano uptake, in comparison with ions, is possibly due to the chemical nature of Co-nano since the particles may interact with proteins present in culture medium on their surface and be more readily taken up by cells (24,36). This type of internalization process due to nano-protein interaction is also suggested by Limbach *et al*. (37), who indicate that the particles could efficiently enter the cells by a Trojan horse-type mechanism (37). Other specific studies are ongoing to understand the intracellular trafficking (interaction with cells, uptake and intracellular distribution) of nanoparticles in *in vitro* systems relevant for human exposure.

Conclusions

In this work, we demonstrated that by adapting standard *in vitro* systems, it is feasible to give a better view of the possible toxicological profile of Co-nano. In fact, our results, taking into consideration also the physicochemical characteristics and the behaviour in culture medium of the nanomaterial studied, showed that Co-nano cytotoxicity, morphological transforming activity and genotoxicity can be assessed.

For cytotoxicity, since for both Co^{2+} and Co-nano we observed a positive effect, we cannot speculate on a real toxicity of Co-nano *per se* but, likely due to a possible synergic effect of ions released in culture medium and/or after its dissolution in cells, as observed from Co-nano. Regarding morphological transforming and genotoxic effects, the data showed a different behaviour. In fact, since no morphological transformation and genotoxicity by micronucleus was observed for Co^{2+}, we can speculate that for these particular end points, the toxic mechanisms are mainly triggered by Co-nano. In this context, future studies are planned in order to better understand the mechanisms of Co-nano effects.

Finally, in our opinion, in order to identify any potential impact of nanoparticles on human health, it is essential to investigate fully their toxicological profiles in different *in vitro* and *in vivo* models.

Funding

European Commission, Joint Research Centre, Nanobiosciences Unit, project: 'NanoBioTechnology for Health'.

Acknowledgements

The authors thank Mr Takao Sasaki and Dr Stephane Mornet for their contribution in the characterization of Co-nano.

Conflict of interest statement: None declared.

References

1. Bergamaschi, E., Bussolati, O., Magrini, A., Bottini, M., Migliore, L., Bellucci, S., Iavicoli, I. and Bergamaschi, A. (2006) Nanomaterials and lung toxicity: interactions with airways cells and relevance for occupational health risk assessment. *Int. J. Immunopathol. Pharmacol*., **19**, 3–10.
2. Colvin, V. (2003) The potential environmental impact of engineered nanomaterials. *Nat. Biotechnol*., **21**, 1166–1170.
3. European Commission. The European Strategy for Nanotechnology and the Nanotechnology Action Plan. (http://cordis.europa.eu/nanotechnology/actionplan.htm—accessed 8 July 2009).
4. Hartung, T., Bremer, S., Casati, S. *et al*. (2004) A modular approach to the ECVAM principles on test validity. *Altern. Lab. Anim*., **32**, 467–472.
5. Ponti, J. (2008) In vitro nanotoxicology activities at the Joint Research Centre (JRC). *Nanotoxicology*, **2** (suppl 1), 35.
6. Wang, K., Xu, J. J. and Chen, H. Y. (2005) A novel glucose biosensor based on the nanoscaled cobalt phthalocyanine-glucose oxidase biocomposite. *Biosens. Bioelectron*., **20**, 1388–1396.
7. Yang, M. H., Jiang, J. H., Yang, Y. H., Chen, X. H., Shen, G. L. and Yu, R. Q. (2006) Carbon nanotube/cobalt hexacyanoferrate nanoparticle-biopolymer system for the fabrication of biosensors. *Biosens. Bioelectron*., **21**, 1791–1797.

8. Hartung, T., Bremer, S., Casati, S. *et al*. (2003) ECVAM's response to the changing political environment for alternatives: consequence of the European Union Chemical and Cosmetic Policies. *Altern Lab Anim*, **31**, 473–481.
9. Mazzotti, F., Sabbioni, E., Ghiani, M., Cocco, B., Ceccatelli, R. and Fortaner, S. (2001) In vitro assessment of cytotoxicity and carcinogenic potential of chemicals: evaluation of the cytotoxicity induced by 58 metal compounds in the BALB/3T3 cell line. *Altern Lab Anim*, **29**, 601–611.
10. Ponti, J., Ceriotti, L., Munaro, B., Farina, M., Munari, A., Whelan, M., Colpo, P., Sabbioni, E. and Rossi, F. (2006) Comparison of impedance-based sensors for cell adhesion monitoring and *in vitro* methods for detecting cytotoxicity induced by chemicals. *Altern Lab Anim*, **34**, 515–525.
11. Bertolero, F., Pozzi, G., Sabbioni, E. and Saffiotti, U. (1987) Cellular uptake and metabolic reduction of pentavalent to trivalent arsenic as determinants of cytotoxicity and morphological transformation. *Carcinogenesis*, **8**, 803–808.
12. IARC. (1991) *Monograph on the Evaluation of Carcinogenic Risk to Humans. Chromium, Nickel and Welding*. International Agency for Research on Cancer, Lyon, France, 49.
13. Elias, Z., Poirot, O., Baruthio, F. and Daniere, M. C. (1991) Role of solubilized chromium in the induction of morphological transformation of Syrian hamster embryo (SHE) cells by particulate chromium(VI) compounds. *Carcinogenesis*, **12**, 1811–1816.
14. IARC/NCI/EPA Working-Group (1985) Cellular and molecular mechanisms of cell transformation and standardization of transformation assays of established cell lines for the prediction of carcinogenic chemicals: overview and recommended protocols. *Cancer Res*., **45**, 2395–2399.
15. Heidelberger, C., Freeman, A. E., Pienta, R. J. *et al*. (1983) Cell transformation by chemical agents—a review and analysis of the literature: a report of the U.S. Environmental Protection Agency Gene-Tox Program. *Mutat. Res*., **114**, 283–385.
16. Ponti, J., Munaro, B., Fischbach, M., Hoffmann, S. and Sabbioni, E. (2007) An optimized data analysis for the Balb/c3T3 cell transformation assay and its application to metal compounds. *Int. J. Immunpathol. Pharmacol*., **20**, 667–678.
17. Agresti, A. (2002) *Categorical Data Analysis*. 2nd edn. Wiley Interscience, John Wiley & Sons, Inc., Hoboken, NJ, pp. 91.
18. Singh, N. P., McCoy, M. T., Tice, R. R. and Schneider, E. L. (1988) A simple technique for quantisation of low levels of DNA damage in individual cells. *Exp. Cell Res*., **175**, 184–191.
19. Duez, P., Dehon, G., Kumps, A. and Dubois, J. (2003) Statistic of Comet assay: a key to discriminate between genotoxic effects. *Mutagenesis*, **18**, 159–166.
20. Surralles, J., Xamena, N., Creus, A., Catalan, J., Norppa, H. and Marcos, R. (1995) Induction of micronuclei by five pyrethroid insecticides in whole-blood and isolated human lymphocyte cultures. *Mutat. Res*., **341**, 169–184.
21. Donaldson, K. and Tran, C. L. (2002) Inflammation caused by particles and fibers. *Inhal. Toxicol*., **14**, 5–27.
22. Brown, D. M., Wilson, M. R., MacNee, W., Stone, V. and Donaldson, K. (2001) Size-dependent proinflammatory effects of ultrafine polystyrene particles: a role for surface area and oxidative stress in the enhanced activity of ultrafines. *Toxicol. Appl. Pharmacol*., **175**, 191–199.
23. Tran, C. L., Buchanan, D., Cullen, R. T., Searl, A., Jones, A. D. and Donaldson, K. (2000) Inhalation of poorly soluble particles. II. Influence of particle surface area on inflammation and clearance. *Inhal. Toxicol*., **12**, 1113–1126.
24. Oberdorster, G., Oberdorster, E. and Oberdorster, J. (2005) Nanotoxicology: an emerging discipline evolving from studies of ultrafine particles. *Environ. Health Persp*., **113**, 823–839.
25. Sabbioni, E., Ponti, J., Del Torchio, R., Farina, M., Fortaner, S., Munaro, B., Sasaki, T. and Rossi, F. (2006) Recherche in vitro sur la toxicologie des nanoparticules au Joint Research Center. *Medecine Nucleaire—Imagerie Fonctionelle et Metabolique*, **30**, 1.
26. Salata, O. V. (2004) Applications of nanoparticles in biology and medicine. *J. Nanobiotechnology*, **2**, 3.
27. Soto, K., Garza, K. M. and Murr, L. E. (2007) Cytotoxic effects of aggregated nanomaterials. *Acta Biomater*., **3**, 351–358.
28. Raja, P. M., Connolley, J., Ganesan, G. P., Ci, L., Ajayan, P. M., Nalamasu, O. and Thompson, D. M. (2007) Impact of carbon nanotube exposure, dosage and aggregation on smooth muscle cells. *Toxicol. Lett*., **28**, 51–63.
29. IARC. (1991) Chlorinated drinking-water chlorination by-products some other halogenated compounds cobalt and cobalt compounds. *IARC Monogr. Eval. Carcinog. Risks Hum*., **52**, 1–544.
30. Kuo, C. Y., Wong, R. H., Lin, J. Y., Lai, J. C. and Lee, H. (2006) Accumulation of chromium and nickel metals in lung tumors from lung cancer patients in Taiwan. *J. Toxicol. Environ. Health A*, **69**, 1337–1344.
31. Lison, D., De Boeck, M., Verougstraete, V. and Kirsch-Volders, M. (2001) Update on the genotoxicity and carcinogenicity of cobalt compounds. *Occup. Environ. Med*., **58**, 619–625.
32. De Boeck, M., Lombaert, N., De Backer, S., Finsy, R., Lison, D. M. and Kirsch-Volders, M. (2003) In vitro genotoxic effects of different combinations of cobalt and metallic carbide particles. *Mutagenesis*, **18**, 177–186.
33. Lison, D., Carbonnelle, P., Mollo, L., Lauwerys, R. and Fubini, B. (1995) Physicochemical mechanism of the interaction between cobalt metal and carbide particles to generate toxic activated oxygen species. *Chem. Res. Toxicol*., **8**, 600–606.
34. De Boeck, M., Kirsch-Volders, M. and Lison, D. (2003) Cobalt and antimony: genotoxicity and carcinogenicity. *Mutat. Res*., **533**, 135–152.
35. Colognato, R., Bonelli, A., Ponti, J., Farina, M., Bergamaschi, E., Sabbioni, E. and Migliore, L. (2008) Comparative genotoxicity of cobalt nanoparticles and ions on human peripheral leukocytes in vitro. *Mutagenesis*, **23**, 1–6.
36. Oberdörster, G., Maynard, A., Donaldson, K. *et al*. (2005) A report from the ILSI Research Foundation/Risk Science Institute National Toxicity Screening Working Group. Principles for characterizing the potential human health effects from exposure to nanomaterials: elements of a screening strategy. *Part. Fibre Toxicol*., **6**, 2–8.
37. Limbach, L. K., Wick, P., Manser, P., Grass, R. N., Bruinink, A. and Stark, W. J. (2007) Exposure of engineered nanoparticles to human lung epithelial cells: influence of chemical composition and catalytic activity on oxidative stress. *Environ. Sci. Technol*., **41**, 3791–3792.

Received on February 15, 2008; revised on May 6, 2009; accepted on May 28, 2009